First observation of [Pu6(OH)4O4]12+ cluster during the hydrolytic formation of PuO2 nanoparticles using H/D kinetic isotope effect

Manon Cot-Auriol, Matthieu Virot, Thomas Dumas, Olivier Diat, Denis Menut, Philippe Moisy, Sergey Nikitenko

COMMUNICATION

First observation of $[Pu_6(OH)_4O_4]^{12+}$ cluster during the hydrolytic formation of PuO_2 nanoparticles using H/D kinetic isotope effect

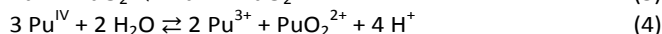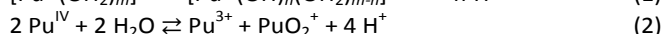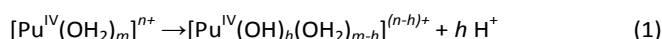Manon Cot-Auriol,[a] Matthieu Virot,*[a] Thomas Dumas,[b] Olivier Diat,[a] Denis Menut,[c]

Philippe Moisy[b] and Sergey I. Nikitenko[a]

New insights are provided about the formation mechanism of PuO2 nanoparticles (NPs) by investigating an unprecedented kinetic isotope effect observed during their hydrolytic synthesis in H2O or D2O and attributed to OH/OD zero point energy difference. The signature of a Pu(IV) oxo-hydroxo hexanuclear cluster, appearing as an important intermediate during the formation of the 2 nm PuO2 NPs (synchrotron SAXS/XAS), is further revealed indicating that their formation is controlled by H-transfer reactions occurring during hydroxo to oxo-bridge conversions.

Anthropogenic activities significantly contributed in the release of plutonium in the environment and related colloids are currently interrogated about their role in the migration of radioactivity in aquatic systems.[1–4] Pu chemistry in aqueous solution involves complex processes including redox/disproportionation, hydrolysis and complexation reactions that can particularly compete for the (+IV) redox state.[5,6] Pu(IV) is indeed highly prone to hydrolysis and the subsequent formation of oligomers that further condensate yielding intrinsic colloids and/or precipitates, even in acidic conditions.[7–9] Meanwhile, disproportionation of Pu(IV) and Pu(V) significantly contribute in the accumulation of ionic Pu(VI), Pu(V) and Pu(III) species during their formation.[7,8,10] While recent investigations reach a consensus in describing intrinsic Pu colloids as *ca.* 2 nm PuO2-like NPs, much less is known about their formation mechanism.[11–14] The description of Pu oxo-hydroxo clusters, with a characteristic size situated somewhere between the ones of ionic and colloidal species of Pu, highlighted the relation between their core structures revealing some striking similarities with bulk PuO2. This suggested that bigger clusters could be formed from the assembly of those smaller molecular fragments.[5,15–18] A better knowledge about the underlying mechanism would help in understanding the behaviour of these species in environmental context and pave the way for pioneering approaches devoted to the control of the size-property relationship of Pu nanomaterials.[13] Kinetic isotope effect (KIE) can be observed when comparing reaction rates in H2O and D2O.[19] Primary KIE originates from the cleavage of O-H bonds and differs from solvent isotope effect which is related to differences in the physico-chemical properties of H2O and D2O solvents (pKw, polarity, viscosity…).[20] In this work, H/D KIE was explored to probe the formation mechanism of colloidal PuO2 NPs.

The formation kinetics of intrinsic Pu(IV) colloids was monitored by Vis-NIR absorption spectroscopy (Fig. 1a) by diluting a Pu(IV) concentrated solution in H2O or D2O (ESI). It is important to mention that the pH (pD) of the studied solutions is imposed by the acidity of the added Pu(IV) solution aliquot (the slight pKw difference resulting from self-ionization of H2O and D2O is not responsible for KIE described below, ESI). After a few minutes in H2O, the characteristic electronic signature from Pu(IV) colloids (resulting from Pu(IV) hydrolysis, Eq. 1) was observed with a main absorption band located around 616 nm and several others at 578, 688 and 735 nm.[21] The sharp absorption band at 830 nm was attributed to the additional presence of Pu(VI) in solution (PuO2^{2+} form, less than *ca.* 3% of total Pu) resulting from Pu(IV) disproportionation (Eq. 2-4).[9,22]

$$[Pu^{IV}(OH_2)_m]^{n+} \rightarrow [Pu^{IV}(OH)_h(OH_2)_{m-h}]^{(n-h)+} + h\ H^+ \quad (1)$$

$$2\ Pu^{IV} + 2\ H_2O \rightleftharpoons Pu^{3+} + PuO_2^+ + 4\ H^+ \quad (2)$$

$$Pu^{IV} + PuO_2^+ \rightleftharpoons Pu^{3+} + PuO_2^{2+} \quad (3)$$

$$3\ Pu^{IV} + 2\ H_2O \rightleftharpoons 2\ Pu^{3+} + PuO_2^{2+} + 4\ H^+ \quad (4)$$

[a.] ICSM, Univ Montpellier, CEA, CNRS, ENSCM, Marcoule, France.
 matthieu.virot@cea.fr
[b.] CEA, DES, ISEC, DMRC, Univ Montpellier, Marcoule, France.
[c.] Synchrotron SOLEIL, MARS beamline, l'Orme des Merisiers, Saint Aubin BP 48,
 91192 Gif-sur-Yvette, France.
† Footnotes relating to the title and/or authors should appear here.
Electronic Supplementary Information (ESI) available: additional spectra, experimental details and methods. See DOI: 10.1039/x0xx00000x
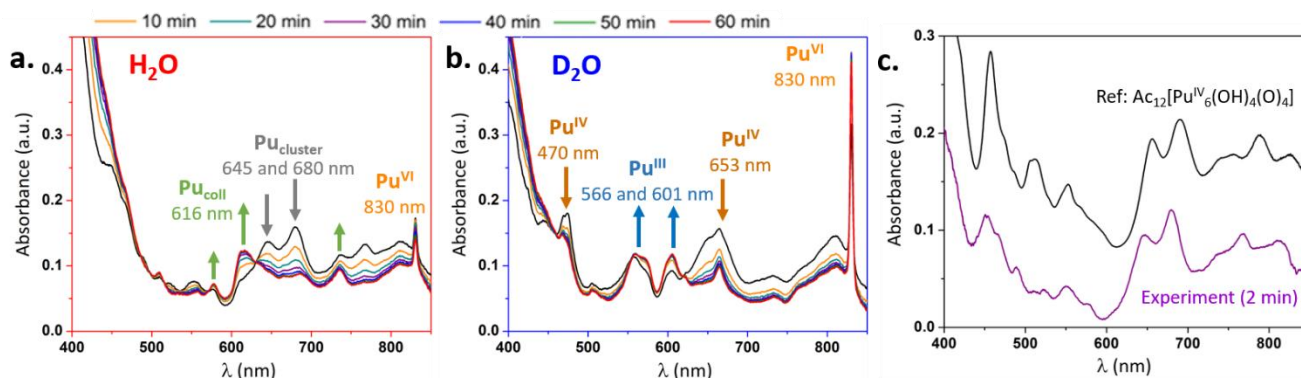
Fig. 1. Vis-NIR absorption spectra acquired during the synthesis of Pu(IV) colloids in (a) H_2O and (b) D_2O in the 2-60 min range. (c) Vis-NIR absorption spectrum acquired 2 min after dispersion of concentrated Pu(IV) in H_2O (without contributions of Pu(III), Pu(VI) and Pu_{coll}) compared to Pu(IV) acetate hexanuclear cluster, with courtesy of C. Tamain.[15]

Pu(III) concentration should be *ca.* twice the one of Pu(VI) according to Eq. 2-4 but it is hardly observed due to low molar coefficient (33 $M^{-1} \cdot cm^{-1}$) and the superposition of the various transitions in the 600-700 nm spectral range. The absorption spectra acquired in D_2O for similar other conditions evolved differently. In particular, indisputable signatures of Pu(IV) (hydrolyzed forms, 470 nm and 653 nm) and Pu(III) (Pu^{3+} form at 601 nm and 566 nm) were observed contrasting with experiments carried out in H_2O.[9,22] Also, the determined amount of Pu(VI) at 830 nm was much higher in D_2O (*ca.* 15% of total Pu) (Fig. 1b). After several weeks and despite strong kinetic differences, both aged H_2O and D_2O solutions of Pu converged to stable Pu(IV) intrinsic colloids as evidenced by characteristic absorption spectra (Fig. S3, ESI). Such a behaviour is attributed to KIE occurring during Pu(IV) hydrolysis and leading to slowdown of Pu colloid formation.[23,24]

A closer look at the electronic spectra acquired during the first hour in H_2O medium (Fig. 1a) allows observing an original transient species with principal absorption bands located at 680 and 645 nm. The spectrum appears directly after Pu(IV) dilution in H_2O (spectra at 2 min) and decreases in absorbance with time while the characteristic spectra of the Pu colloids appear. An isobestic point observed at 630 nm suggests a two-component conversion. Deconvolution studies which consisted in the subtraction of reference spectra (Pu(III-VI) and Pu_{coll}) from the experimental ones revealed an unprecedented signature (Fig. 1c) which offered striking similarities with a recently described oxo-hydroxo hexanuclear core of a Pu(IV) cluster $[Pu_6(OH)_4O_4]^{12+}$ decorated by acetate or DOTA ligands.[15,16] Slight differences between both spectra were attributed to the decoration of the latter with acetate ligands (on-going efforts aim at stabilizing this specie during Pu(IV) colloid synthesis). A similar observation in D_2O appeared more complicated due to the important contribution of other Pu ionic species originated from Pu(IV) disproportionation and hydrolysis. The deconvoluted spectrum revealed a noisy signal most likely attributed to low concentrated Pu(IV) polynuclear cores including the hexamer or Pu(IV) hydrolysed species (Fig. S4, ESI).

Kinetic curves were extracted from deconvolution (approach described in ESI) studies to understand the observed reactivity differences during the first minutes. Fig. 2a and 2b confirm the more important disproportionation of Pu(IV) (with a stronger accumulation of ionic Pu(VI) and Pu(III) in solution) and the lower concentration of the Pu cluster intermediate in D_2O medium. Pu(VI) concentration is twice the one of Pu(III) in agreement with the Eq. 4. Note that Pu(V) was not observed during deconvolution but its presence in the process can't be excluded. In both media, Pu(VI) quickly accumulated in solution during *ca.* 30 min before slowly decreasing with time (Fig. 2c). The initial accumulation rate of Pu(VI) was found to be slightly higher in D_2O than in H_2O (20.1 *vs.* 5.2 $mM \cdot h^{-1}$, respectively).

After ca. 30 min, Pu(VI) consumption was explained by its reaction with Pu(III) (*i.e.* Pu(IV) comproportionation). A first order reaction law was used on Pu(VI) to compare both kinetics in agreement with the work of Rabideau and Kline (Eq. 2, ESI).[25] It is interesting to note that the logarithm function only fitted in the 30-120 min range for H_2O medium which was attributed to the evolution of Pu species during comproportionation and a possible alternative mechanism when Pu(VI) and Pu(III) show a very low concentration in solution.[9] Fig 2c evidences the significantly higher reduction rate of Pu(VI) observed in H_2O ($k^H(-Pu^{VI})/k^D(-Pu^{VI})$ = 6.8). The consumption of Pu(III) was not considered due to its low absorbance and the interferences with the spectra of other Pu species. Deconvolutions also allowed to estimate the formation kinetics of Pu(IV) colloids at ca. 616 nm (Fig. 2d). Assuming a first order formation rate on the colloid (Eq. 5, ESI), it was confirmed that the latter accumulates at a much lower rate in D_2O. The calculated ratio of the colloid formation kinetic constants $k^H(Pu_{coll})/k^D(Pu_{coll})$ equalled 7.4.

Synchrotron measurements allowed the quasi-simultaneous characterization of the aged (> 1 month) colloids by small-angle X-ray scattering (SAXS) and X-ray absorption spectroscopy (XAS) without altering the nature of the samples (Fig. S5, ESI). Normalized SAXS diagrams exhibited similar scattering profiles in both cases (Fig. 3), characteristic from sharp interfaces typical for 3D dense particles.[26] Considering a simple model of spherical and homogeneous NPs with a slight polydispersity (0.15), the data adjustment provided a slightly higher radius for the colloid formed in D_2O (1.1 ± 0.1 nm *vs.* 0.9 ± 0.1 nm in H_2O). The determined scattering length density (*ca.*

COMMUNICATION

69 10^{10} cm^{-2}) and the volume fraction were very close to the estimated parameters (Table S3, ESI). This simple model, with few but consistent parameters, is well representative of the scattering signal variation in absolute scale.

faster disproportionation of Pu(IV) in H_2O which is not the case in our study (Fig. 2c). By contrast, the KIE can be explained by the zero point energy difference between O-H and O-D bonds (ΔE = 5.89 kJ·mol^{-1}).[19,34] As a consequence, more energy is
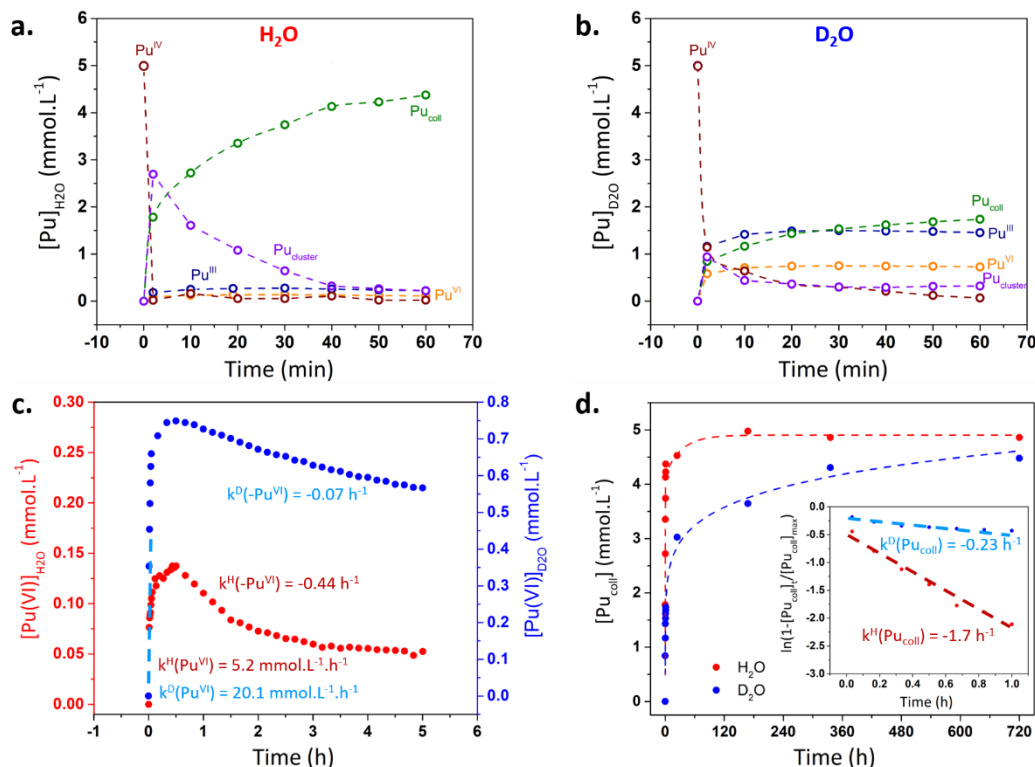

Fig. 2. (a,b) Kinetics related to Pu species in H_2O and D_2O after deconvolution. (c) Evolution of Pu(VI) concentration during the synthesis of Pu(IV) colloids in H_2O and D_2O. A special care should be given to scale bar differences. Dashed lines represent linear regressions used to determine kinetic rates (corresponding values given in ESI). (d) Evolution of the colloid absorbance (λ = 616 nm) as a function of time after deconvolution of the absorbance spectra. Insert: plot of the natural logarithm of Pu colloid absorbance against time.

X-ray absorption near-edge structure (XANES) spectra acquired at the Pu L_3 edge on the colloids formed in both media exhibited a white line (18067 eV) at similar positions, agreeing with the strong predominance of the (+IV) oxidation state for Pu (Fig. S6, ESI).[27,28] A slight difference observed on the spectra at *ca.* 18080 eV was attributed to the significant contribution of Pu(VI) ions in D_2O. In order to compare the data obtained in H_2O and D_2O, a XAS spectrum of Pu(VI) was subtracted from the experimental data obtained in D_2O.[27,28] The resulting EXAFS spectrum was found to be similar to the one acquired in H_2O (Fig. S6, ESI). Both FT showed two main peaks at R-φ = *ca.* 1.84 and 3.68 Å, agreeing with Pu(IV) colloids[11,26,29] and crystalline bulk PuO_2 (CFC, Fm-3m).[7,30] The structural parameters of the fits demonstrated that local structures of the colloids prepared in this study are similar and close to bulk PuO_2 (Table S5, ESI).

As a first conclusion, the observed strong KIE only shows little influence on the final shape, size and local structure of the NPs which can be described as 2 nm spherical NPs with a PuO_2-like local structure.[7,11,14,26,31,32] The physico-chemical property differences reported for H_2O and D_2O at room temperature and originating solvent isotope effects in some cases cannot explain the observed KIE.[20] As well, it has been demonstrated that quantum tunnelling observed for electron or H atom transfer is more important in H_2O than in D_2O.[33] Such a phenomenon could have been invoked to explain a

required to break the latter bonds favouring disproportionation of Pu(IV) in D_2O medium instead of the cluster formation. Therefore, O-H bond ruptures appear as rate-limiting steps during the colloid formation. The calculated theoretical isotopic separation factor $\alpha_{(H/D)}$ equals 10.6 at T = 300 K (Eq. 6, ESI) which is in good agreement with the k^H/k^D ratios observed for Pu(VI) reduction and Pu colloid formation. Interestingly, kinetic studies related to hydrolysis in D_2O are scarce in the literature. We only found one recent publication describing the hydrolysis of Ce(IV) and subsequent formation of CeO_2 NPs with a close ratio k^H/k^D = 10.[35]

It has been argued that Pu(IV) disproportionation is preceded by Pu(IV) ions hydrolyses and the generation of polynuclear hydroxo complexes.[36] The slightly higher accumulation rates observed for Pu(VI) in D_2O after disproportionation suggest that hydrolysis of Pu(IV) (Eq. 1) is poorly affected by KIE. By contrast, both the cluster core and Pu colloid formation are limited in D_2O. The presence of
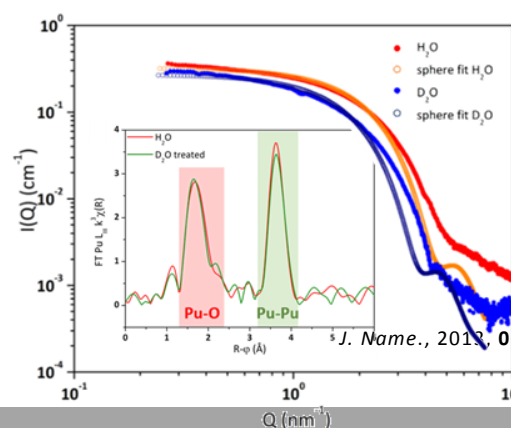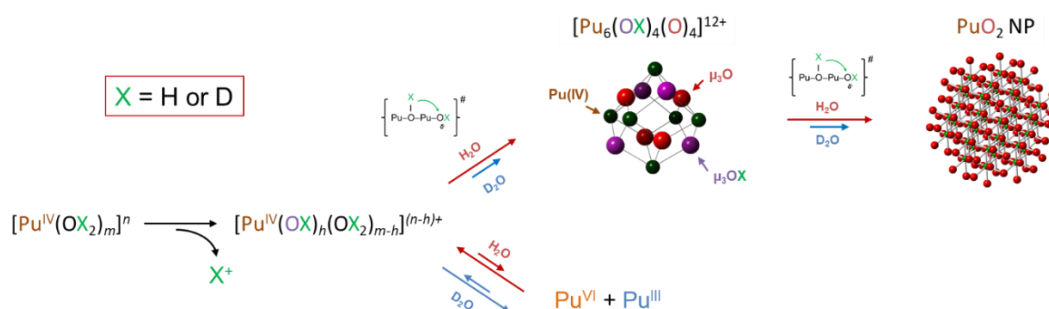

Fig. 3. SAXS diagrams of Pu(IV) colloids formed in H_2O and D_2O and corresponding fits. Inset: k^3-weighted FT for Pu(IV) colloids (H_2O and D_2O, without Pu(VI) contribution).

Scheme 1. Scheme of the formation mechanism of the colloidal PuO_2 nanoparticles.

hydroxo-bridges in the hexanuclear cluster and their absence in the final oxo-NP demonstrates that the Pu colloid formation involves a succession of olation and oxolation reactions confirming that PuO_2 NPs formation is limited by H-atom transfer reactions (scheme 1).[6,18] This observation further discards classical crystal nucleation theory for PuO_2 NPs in aqueous media where crystal growth occurs through the addition of monomeric units[37] but rather suggests the stacking of metastable and structurally well-defined oxo-hydroxo Pu(IV) clusters as a favoured mechanism,[17] as also suggested for U(IV) cluster analogues.[38,39]

Conflicts of interest

There are no conflicts to declare.

References

1   G. J.-P. Deblonde, A. B. Kersting and M. Zavarin, *Commun. Chem.*, 2020, **3**, 167.
2   A. Yu. Romanchuk, I. E. Vlasova and S. N. Kalmykov, *Front. Chem.*, 2020, **8**, 630.
3   A. B. Kersting, *Inorg. Chem.*, 2013, **52**, 3533–3546.
4   E. L. Tran, O. Klein-BenDavid, N. Teutsch and N. Weisbrod, *Environ. Sci. Technol.*, 2015, **49**, 13275–13282.
5   L. Soderholm, P. M. Almond, S. Skanthakumar, R. E. Wilson and P. C. Burns, *Angew. Chem. Int. Ed.*, 2008, **47**, 298–302.
6   D. A. Costanzo, R. E. Biggers and J. T. Bell, *J. Inorg. Nucl. Chem.*, 1973, **35**, 609–622.
7   J. Rothe, C. Walther, M. A. Denecke and Th. Fanghänel, *Inorg. Chem.*, 2004, **43**, 4708–4718.
8   V. Neck and J. I. Kim, *Radiochim. Acta*, 2001, **89**, 1–16.
9   D. L. Clark, S. S. Hecker, G. D. Jarvinen and M. P. Neu, in *The chemistry of the actinide and transactinide elements*, Springer Netherland, Drodrecht, 2006, pp. 813–1264.
10 C. Walther, H. R. Cho, C. M. Marquardt, V. Neck, A. Seibert, J. I. Yun and T. Fanghänel, *Radiochim. Acta*, 2007, **95**, 7–16.
11 E. Dalodière, M. Virot, V. Morosini, T. Chave, T. Dumas, C. Hennig, T. Wiss, O. Dieste Blanco, D. K. Shuh, T. Tyliszcak, L. Venault, P. Moisy and S. I. Nikitenko, *Sci. Rep.*, 2017, **7**, 43514.
12 M. Virot, T. Dumas, M. Cot-Auriol, P. Moisy and S. I. Nikitenko, *Nanoscale Adv.*, 2022, In press.
13 E. Gerber, A. Yu. Romanchuk, S. Weiss, A. Kuzenkova, M. O. J. Y. Hunault, S. Bauters, A. Egorov, S. M. Butorin, S. N. Kalmykov and K. O. Kvashnina, *Environ. Sci.: Nano*, 2022, **9**, 1509–1518.
14 E. Gerber, A. Yu. Romanchuk, I. Pidchenko, L. Amidani, A. Rossberg, C. Hennig, G. B. M. Vaughan, A. Trigub, T. Egorova, S. Bauters, T. Plakhova, M. O. J. Y. Hunault, S. Weiss, S. M. Butorin,
15 G. Chupin, C. Tamain, T. Dumas, P. L. Solari, P. Moisy and D. Guillaumont, *Inorg. Chem.*, 2022, **61**, 4806–4817.
16 C. Tamain, T. Dumas, D. Guillaumont, C. Hennig and P. Guilbaud, *Eur. J. Inorg. Chem.*, 2016, **2016**, 3536–3540.
17 K. E. Knope and L. Soderholm, *Inorg. Chem.*, 2013, **52**, 6770–6772.
18 G. E. Sigmon and A. E. Hixon, *Chem. Eur. J.*, 2019, **25**, 2463–2466.
19 S. Scheiner and M. Čuma, *J. Am. Chem. Soc.*, 1996, **118**, 1511–1521.
20 G. Swain and F. W. Bader, *Tetrahedron*, 1960, **10**, 182–199.
21 M. H. Lloyd and R. G. Haire, *Radiochim. Acta*, 1978, **25**, 139–148.
22 D. Jebaraj Mahildoss and T. N. Ravi, *J. Radioanal. Nucl. Chem.*, 2012, **294**, 87–91.
23 S. W. Rabideau, *J. Am. Chem. Soc.*, 1953, **75**, 798–801.
24 S. W. Rabideau and R. J. Kline, *J. Phys. Chem.*, 1960, **64**, 680–682.
25 S. W. Rabideau and R. J. Kline, *J. Phys. Chem.*, 1958, **62**, 617–620.
26 C. Micheau, M. Virot, S. Dourdain, T. Dumas, D. Menut, P. L. Solari, L. Venault, O. Diat, P. Moisy and S. I. Nikitenko, *Environ. Sci.: Nano*, 2020, **7**, 2252–2266.
27 T. Vitova, I. Pidchenko, D. Fellhauer, T. Pruessmann, S. Bahl, K. Dardenne, T. Yokosawa, B. Schimmelpfennig, M. Altmaier, M. Denecke, J. Rothe and H. Geckeis, *Chem. Commun.*, 2018, **54**, 12824–12827.
28 S. D. Conradson, D. L. Clark, M. P. Neu, W. Runde and C. D. Tait, *Los Alamos Sci.*, 2000, **26**, 418–421.
29 C. Ekberg, K. Larsson, G. Skarnemark, A. Ödegaard-Jensen and I. Persson, *Dalton Trans.*, 2013, **42**, 2035–2040.
30 A. Kuzmin and J. Chaboy, *IUCrJ*, 2014, **1**, 571–589.
31 M. Altmaier, X. Gaona and D. Fellhauer, in *Plutonium Handbook*, American Nuclear Society, La Grange Park, IL, USA, D.A.G. D.L. Clark, R.J. Hanrahan Jr., 2019, vol. 3.
32 L. Bonato, M. Virot, T. Dumas, A. Mesbah, E. Dalodière, O. Dieste Blanco, T. Wiss, X. Le Goff, M. Odorico, D. Prieur, A. Rossberg, L. Venault, N. Dacheux, P. Moisy and S. I. Nikitenko, *Nanoscale Adv.*, 2020, **2**, 214–224.
33 T. Kumagai, M. Kaizu, S. Hatta, H. Okuyama, T. Aruga, I. Hamada and Y. Morikawa, *Phys. Rev. Lett.*, 2008, **100**, 166101.
34 M. Ceriotti, W. Fang, P. G. Kusalik, R. H. McKenzie, A. Michaelides, M. A. Morales and T. E. Markland, *Chem. Rev.*, 2016, **116**, 7529–7550.
35 N. W. Pettinger, R. E. A. Williams, J. Chen and B. Kohler, *Phys. Chem. Chem. Phys.*, 2017, **19**, 3523–3531.
36 J. M. Haschke, *J. Nucl. Mater.*, 2007, **362**, 60–74.
37 J. De Yoreo, *Nature Mater.*, 2013, **12**, 284–285.

38 L. Chatelain, R. Faizova, F. Fadaei-Tirani, J. Pécaut and M. Mazzanti, *Angew. Chem. Int. Ed.*, 2019, **58**, 3021–3026.
39 N. P. Martin, C. Volkringer, N. Henry, X. Trivelli, G. Stoclet, A. Ikeda-Ohno and T. Loiseau, *Chem. Sci.*, 2018, **9**, 5021–5032.

38 L. Chatelain, R. Faizova, F. Fadaei-Tirani, J. Pécaut and M.